

Application of Superconducting Fault Current Limiter as a Virtual Inertia for DC Distribution Systems

DOAA M. YEHIA¹ AND IBRAHIM B. M. TAHA²

¹Department of Electrical Power and Machines Engineering, Faculty of Engineering, Tanta University, Tanta 31511, Egypt

²Department of Electrical Engineering, College of Engineering, Taif University, Taif 21944, Saudi Arabia

Corresponding author: Doaa M. Yehia (dmyehia@f-eng.tanta.edu.eg)

This work was supported by Taif University Researchers Supporting Project (TURSP-2020/61), Taif University, Taif, Saudi Arabia.

ABSTRACT DC distribution systems can provide effective solutions for integrating renewable energy sources in future power systems. The low inertia of the DC distribution system causes several problems regarding stability and fault response. For stability, this low inertia represents a major cause for instability and voltage oscillations, especially with constant power loads. For fault response, the low inertia results in very high fault currents with a significant rate of rising and limited damping. This study aims to use superconducting fault current limiter (SFCL) as a virtual inertia for DC distribution systems under various disturbances and fault conditions. The system description and modeling are first presented, including the detailed dynamics of SFCL. The stability analysis for the DC system is carried out using the Hurwitz criterion, from which the suitable range of SFCL resistance is identified. Considering this range and fault current limitation, an SFCL resistance of 1.5 Ω is adopted. The whole system is implemented using PSCAD/EMTDC software. A series of case studies are investigated to validate the effectiveness of SFCL in strengthening the inertia of the DC system. These case studies include sudden variations in supply voltage, sudden load changes, and faults. SFCL could successfully suppress voltage oscillations, keep voltage stability, and limit fault currents.

INDEX TERMS DC distribution system, superconducting fault current limiter, virtual inertia, voltage stability, voltage oscillations, faults.

I. INTRODUCTION

In recent years, the demand for electrical power has been dramatically increased all over the world. It was coincided with an increasing trend in fuel consumption [1], causing a subsequent increase in carbon emissions [2]. So, there are large efforts exerted by electrical utilities to increase the penetration of renewable energy sources in electrical grids.

In this regard, the DC distribution system facilitates renewable energy integration due to the inherent DC characteristics of most renewable energy sources and energy storage devices [3]. In addition, the DC distribution system provides high reliability and low power losses and doesn't necessitate reactive power control or frequency synchronization. Thus, such DC distribution systems were expanded in various scales starting from universal DC distribution system towards DC microgrids and DC nano-grids [4], [5]. The main challenge

in DC distribution systems is their low inertia making them vulnerable to instability, voltage oscillations, and high fault current levels.

Regarding instability and voltage oscillations, they are mainly originated with constant power loads (CPLs) [6]–[8]. The dynamics of CPLs are nonlinear, and their incremental impedance is negative. These both effects cause destabilizing action and sometimes limit the amount of power transferred to the load [9]. The DC voltage is considered the main indicator for DC system instability.

The most widely used sources in DC distribution systems are photovoltaic (PV) systems and battery energy storage systems. PV systems have no inertial response due to the absence of rotational mass and stored kinetic energy. In order to provide such inertial response, PV systems are required to operate below their maximum power point [10], [11], which is not desired from the economic viewpoint. Battery energy storage systems can provide virtual inertia response through proper control, but this eventually reduces the battery lifetime

The associate editor coordinating the review of this manuscript and approving it for publication was Amedeo Andreotti¹.

due to fast variations in DC voltage. It is important to point out that providing virtual inertia response will enable to increase the penetration level of renewable energy sources in DC distribution systems.

On the other hand, several studies analyzed instability in DC distribution systems and proposed various inertia control methods to mitigate this instability [12]–[14]. Most proposed methods require controllable actions, either linear or nonlinear, by the DC-DC converters at the consumer side, which are unmanaged by the power system operator. In addition, these methods don't contribute to the current limitation in case of faults.

Regarding fault current levels, they are extremely large in DC distribution systems. The low inertia acts towards high rate of rising and limited damping for fault currents [15], [16]. The common way to mitigate the negative impact of high fault currents in DC systems is fast-acting protection schemes through disconnecting the proper unit/units [17], [18]. Nevertheless, this solution hinders the fault ride-through capability of the system [19].

To simultaneously enhance the inertial response and limit fault current levels in DC distribution systems, it is proposed in this paper to use superconducting fault current limiters (SFCLs). SFCLs have succeeded in many applications with DC systems [20]–[22] due to their fast operation once their current attains the critical one. In [20], SFCL has succeeded in reducing current transients either for DC faults or for AC ones. In [21], SFCL could prevent sudden drop in the state of charge for batteries connected to the DC system when a fault occurs, thereby preserving their lifetimes. In [22], SFCL could delay the voltage drop in DC grids following fault occurrence, enabling sufficient time for interruption at lower currents.

The paper is organized as follows. First, the system description and modeling issues are presented. Then, the DC system stability is analyzed using the Hurwitz criterion, and the stability conditions are extracted. Based on this analysis, the suitable current limiting resistance is determined. After that, the performance of SFCL as virtual inertia is evaluated through a series of simulation results. Different disturbances are considered, including sudden variations in supply voltage and sudden load changes. Finally, the behavior of SFCL in limiting fault currents is assessed under system faults.

II. SYSTEM DESCRIPTION AND MODELING

A. DC DISTRIBUTION SYSTEM

The schematic representation of the DC distribution system under study is shown in Fig. 1. It consists of a DC bus feeding CPLs through a transmission line. The DC bus is considered to be fed from various renewable energy sources, either DC sources or AC ones, as well as energy storage devices. The DC transmission line has a length of 400 m with an inductance (L) of 0.1 mH/m and resistance (R) of 0.13 Ω /m. At the load side, a DC capacitor (C) of 150 μ F is used.

Regarding the loads, they can be AC or DC loads. Both types are interfaced to the DC system through proper power electronics converters in order to adjust and maintain the voltage level. Therefore, such converters-based loads behave as constant power loads introducing negative incremental impedance at the load side. The rated voltage of the system is 400 V, and its rated power is 30 kW. SFCL was inserted in series to the transmission line at the load terminals. PSCAD/EMTDC platform was used to model the DC distribution system, SFCL, and CPLs.

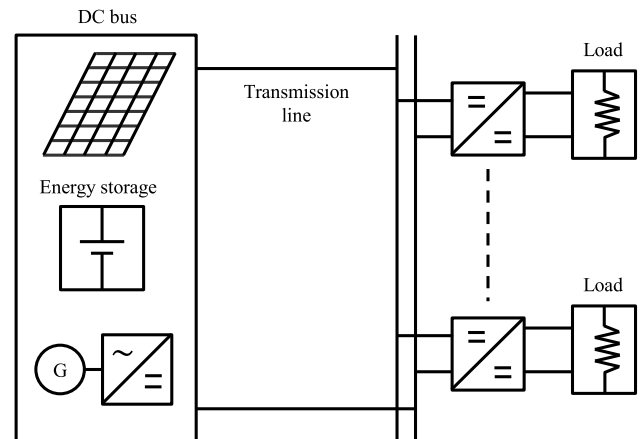


FIGURE 1. Configuration of DC distribution system under study.

B. SFCL MODEL

Resistive-type SFCLs were considered in this study since inductive-type SFCLs can be detrimental to the system's stability. The resistive-type SFCL was modeled so that it represents the nonlinear transition of SFCL from superconducting mode to flux flow mode and resistive mode. This has been performed through using a combination of controlled switch (S), nonlinear resistor (R_{sc}) representing the resistor of superconducting material, and stabilizing resistor (R_{st}) as illustrated in Fig. 2. The controlled switch and nonlinear resistor are controlled for current magnitude, while the stabilizing resistor is modeled as a fixed resistor. The controlled switch is responsible for the transition from and to superconducting mode. In superconducting mode, where the current magnitude is lower than the critical current, this switch is set closed, providing a short path across R_{sc} and R_{st} . Once the current magnitude exceeds above the critical value in case of faults or disturbances, S changes its state to an open state. In this case, the combination of R_{sc} and R_{st} provides the SFCL resistance (R_{SFCL}) according to the thermal and electrical dynamics of R_{sc} . The resistivity ρ_{sc} has a dynamic value depending on the status of current density (J) and temperature (T) as follows [23]:

$$\rho_{sc} = \begin{cases} \frac{E_c}{J_c} \left(\frac{J}{J_c} \right)^n, & \text{Flux flow mode } (J > J_c, T < T_c) \\ f(T), & \text{Conducting mode } (J > J_c, T > T_c) \end{cases} \quad (1)$$

where J_c is the critical current density, T_c is the critical temperature, E_c is the critical electric field, and n is a constant having a value of 20 or higher [24].

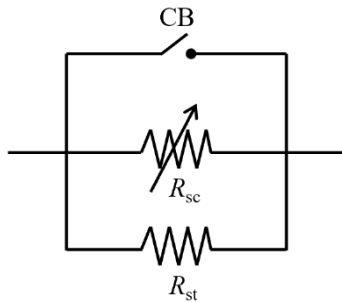


FIGURE 2. Schematic representation of SFCL model.

To account for thermal and electrical dynamics of R_{sc} , its model was developed using thermal and electrical sub-modules. The thermal sub-module is responsible for obtaining thermal dynamics; namely, the temperature variation against current, as illustrated in Fig. 3(a). The amount of heat generated in the superconducting material Q_{sc} and heat dissipated to the surrounding cryogenic system Q_{diss} can be given by [25], [26]:

$$Q_{sc} = \int I_{sc}^2 R_{sc} dt \tag{2}$$

$$Q_{diss} = \int \frac{T(t) - T_a}{\theta_{sc}} dt \tag{3}$$

where I_{sc} is the superconductor current, T_a and $T(t)$ is the cooling and actual temperatures, respectively, and θ_{sc} is the thermal resistance from the superconducting element to the surrounding. The temperature $T(t)$ depends on the difference between the generated and dissipated heats as follows:

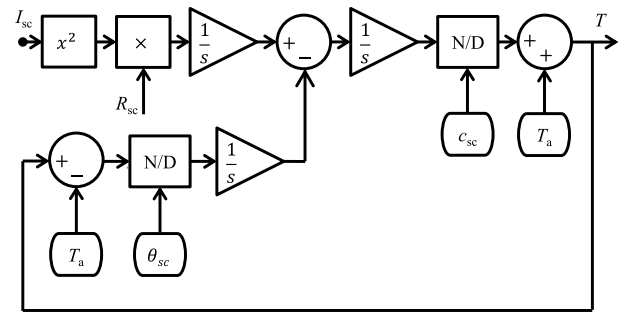
$$T(t) = T_a + \frac{1}{c_{sc}} \int_0^t (Q_{sc} - Q_{diss}) dt \tag{4}$$

where c_{sc} is the heat capacity of the superconductor.

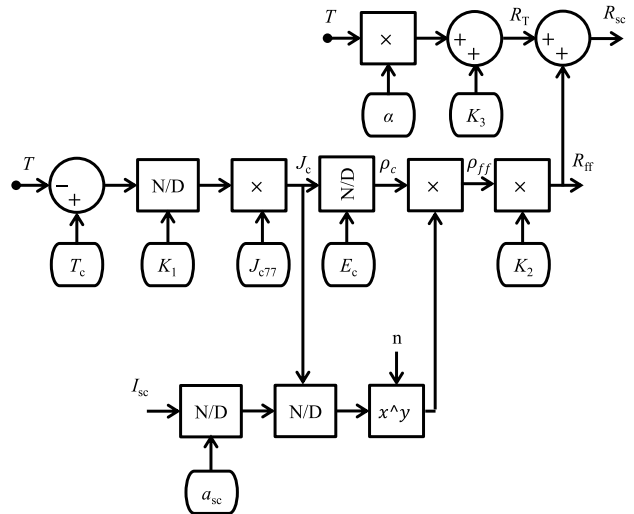
Regarding electrical sub-module, it is aimed to get ρ_{sc} and corresponding R_{sc} using equation (1) in terms of the temperature obtained from thermal sub-module as shown in Fig. 3(b). K_1 , K_2 , K_3 and a are constants and a_{sc} is the cross-section area of the superconductor. The critical current density J_c is obtained as follows:

$$J_c = J_{co} \frac{T_c - T(t)}{T_c - T_a} \tag{5}$$

where J_{co} is the critical current density at the cooling temperature T_a , which is 77 K for liquid nitrogen cooling. R_{sc} is given by the summation of flux flow resistance (R_{ff}) and temperature-dependent resistance (R_T). Since developed R_{sc} is high compared to R_{st} , the total SFCL resistance (R_{SFCL}) will be governed by the stabilizing resistance (R_{st}) value.



(a) Thermal module.



(b) Electrical module.

FIGURE 3. SFCL thermal and electrical modeling.

C. CPL MODEL

The load model was developed considering the concept of voltage sensitivity, which evaluates the dependence of load power p on its voltage v as given by the following equation:

$$p = \frac{P_o}{V_o^\alpha} v^\alpha \tag{6}$$

where P_o and V_o are rated power and voltage, respectively, and α denotes to the voltage sensitivity parameter. The α parameter takes the value of 2, 1, and 0 for constant impedance, constant current, and constant power loads, respectively. So, based on this concept, the load was modeled as a current-dependent nonlinear resistor, whose current is varying to keep its consumed power constant.

III. STABILITY ANALYSIS

Stability analysis for the considered DC system in Fig. 1 was performed using the Hurwitz criterion. The equivalent circuit for the DC distribution system is depicted in Fig. 4. First, let us consider a small disturbance in the load voltage Δv . Under this condition, the power of the CPL in Equation (6) will be given by:

$$p(t) = \frac{P_o}{V_o^\alpha} [v(t)]^\alpha = \frac{P_o}{V_o^\alpha} [V_o + \Delta v]^\alpha \tag{7}$$

Thus, the CPL current $i(t)$ is expressed as:

$$i(t) = \frac{P_o}{V_0^\alpha} (V_o + \Delta v)^{\alpha-1} \quad (8)$$

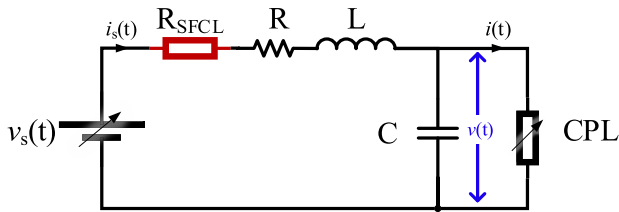


FIGURE 4. Equivalent electrical circuit for the DC distribution system.

By expanding $i(t)$ using Taylor series expansion:

$$i(t) = \frac{P_o}{V_o} + (\alpha - 1) \frac{P_o}{V_o^2} \Delta v + (\alpha - 1)(\alpha - 2) \times \frac{P_o}{2V_o^3} \Delta v^2 + \dots \quad (9)$$

The higher-order terms starting from Δv^2 are very small and can be neglected, making $i(t)$ in the following form:

$$i(t) = \frac{P_o}{V_o} + (\alpha - 1) \frac{P_o}{V_o^2} \Delta v = \frac{P_o}{V_o} + K \Delta v \quad (10)$$

where K is a constant depending on the load ratings and type as follows:

$$K = (\alpha - 1) \frac{P_o}{V_o^2} \quad (11)$$

For CPL, α parameter takes the value of 0, causing K to have a negative value, thus introducing a destabilizing effect. The dynamic equations of the system can be expressed as follows:

$$v_s(t) = R i_s(t) + L \frac{di_s(t)}{dt} + v(t) \quad (12)$$

$$i_s(t) = C \frac{dv(t)}{dt} + i(t) \quad (13)$$

$$i(t) = \frac{P_o}{V_o} + K \Delta v = \frac{P_o}{V_o} + K[v(t) - V_o] \quad (14)$$

where v_s and i_s are the source voltage and current, respectively. By transforming equations (12)-(14) into s-domain:

$$v_s(s) = i_s(s) [R + Ls] + v(s) \quad (15)$$

$$i_s(s) = C s v(s) + i(s) \quad (16)$$

$$i(s) = K v(s) \quad (17)$$

These equations are solved so that the transfer function of the whole system relating the voltage at the load terminal to the source voltage is obtained, and its characteristic equation is given as follows:

$$a_2 s^2 + a_1 s + a_0 \quad (18)$$

where the coefficients of the characteristic equation are deduced as follows:

$$\begin{aligned} a_2 &= LC \\ a_1 &= RC + KL \\ a_0 &= 1 + RK \end{aligned} \quad (19)$$

Using the Hurwitz criterion, the following two conditions have to be fulfilled:

$$\begin{aligned} H_1 &= |a_1| > 0 \\ H_2 &= \begin{vmatrix} a_1 & a_2 \\ 0 & a_0 \end{vmatrix} > 0 \end{aligned} \quad (20)$$

Accordingly, the stability conditions can be expressed as follows:

$$a_2 > 0, \quad a_1 > 0 \text{ and } a_0 > 0 \quad (21)$$

$$H_1 = a_1 > 0 \quad (22)$$

$$H_2 = a_0 a_1 > 0 \quad (23)$$

Equation (19) show that a_2 is greater than zero for all transmission line parameters (L , C). However, coefficient a_0 determines the maximum value of system resistance R , including transmission line resistance and R_{SFCL} . At the same time, the minimum value of R is obtained from a_1 . Therefore, stable operation is obtained for certain line parameters (L , C and R) if transmission line resistance is increased by R_{SFCL} . Based on transmission line parameters depicted in Section II, the minimum and maximum values of SFCL resistance that achieved voltage stability conditions are 0.5Ω and 8Ω , respectively.

IV. RESULTS AND DISCUSSIONS

The rated current of the considered DC system is 75 A. So, the critical current of SFCL was set at 100 A. From the previous section, the range of SFCL resistance that achieved voltage stability conditions was found to be $0.5 - 8 \Omega$. On the other hand, the range of SFCL resistance from 1 to 2Ω was sufficient for the current limitation in DC systems [21], [27]. Accordingly, in this study, SFCL resistance was adopted 1.5Ω . For simulation purposes, the DC bus was modeled as a DC source. The stability of the DC system was investigated for sudden variations in the supply voltage as well as for sudden load changes. In addition, the response of the system against faults was obtained. For all these results, the impact of using SFCL was evaluated.

A. SUDDEN VARIATIONS IN SUPPLY VOLTAGE

Since the DC bus is expected to be fed from renewable energy sources, thus any changes in the environmental conditions will lead to sudden variations in the DC voltage [28]. Two case studies are considered, step down and step up in the supply or source voltage. It is assumed that the voltage varies within $\pm 5\%$ of its nominal value, which corresponds to ± 20 V. Thus, for step down case, the voltage was considered to be decreased from 420 V to 380 V. The instant of sudden voltage variation is 0.5 s as shown in Fig. 5.

Before using SFCL, there is growing oscillations in the load voltage and current directly after the supply voltage steps down as illustrated in Fig. 5. The first peak-to-peak oscillation has been attained after about 1 ms and had a value of 87 V representing about 22% of the nominal DC voltage. In addition, the load current was oscillated with an initial increase from 75 A to 95 A in less than 1 ms. After about 19 ms, the system completely loses the stability. This is attributed to the constant power load that draws larger current with decreasing the voltage. The step up in the supply voltage resulted in less pronounced impact on the DC system.

When using resistive-type SFCL of 1.5 Ω, it is quenched to resistive mode once the load current attains the critical value of 100 A as shown in Fig. 6. This effectively provided a virtual inertia for the system assisting in the suppression of oscillations either in the load voltage or in the load current. SFCL was quenched after about 2 ms of the instant of disturbance for a sudden decrease in supply voltage. In this case, there was no overvoltage occurred at the load side as shown in Fig. 6.

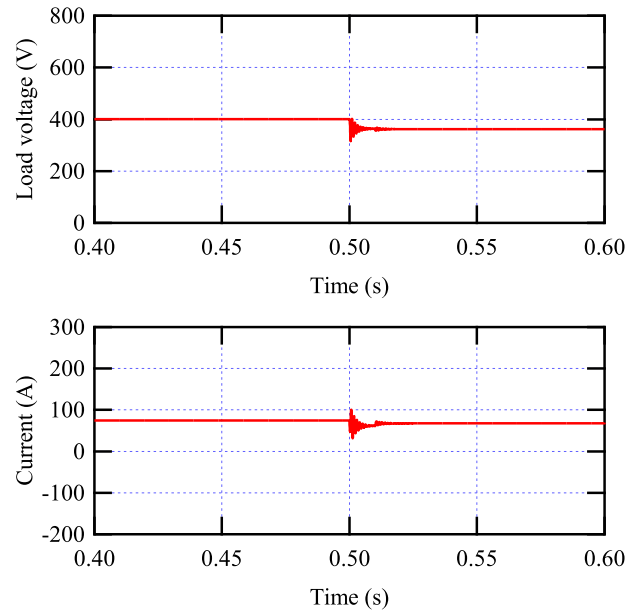


FIGURE 6. Response of DC system for sudden decrease in source voltage after using SFCL.

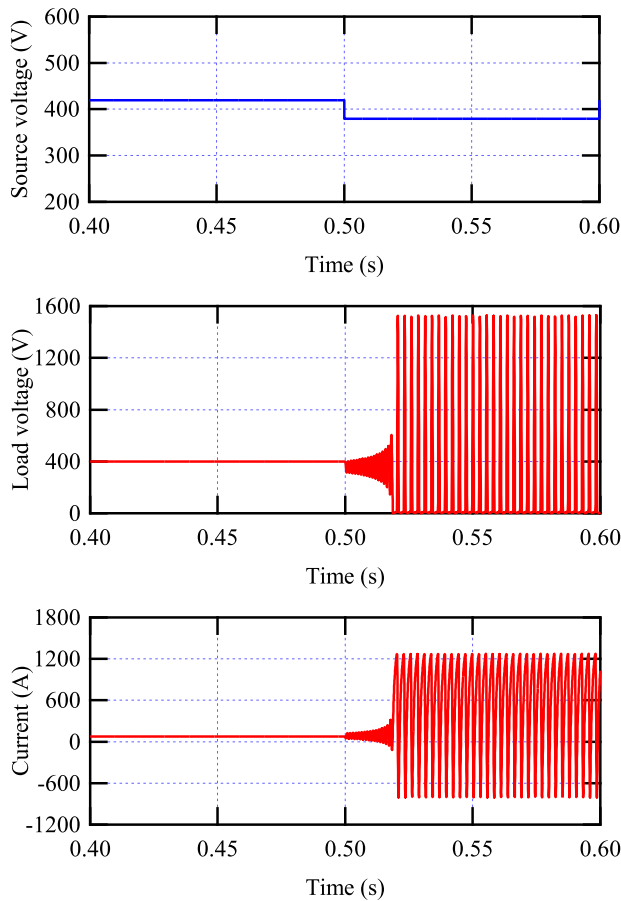


FIGURE 5. Response of DC system for sudden decrease in source voltage before using SFCL.

To compare the results before and after using SFCL, voltage-current characteristics were presented as shown in Fig. 7. Without using SFCL the voltage-current characteristic run away, and the system loses stability. With using

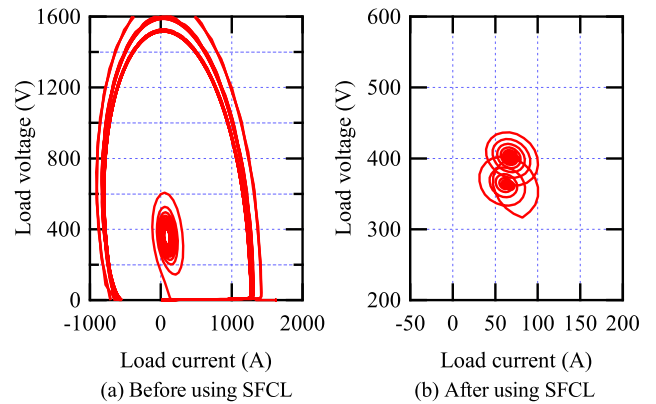


FIGURE 7. Voltage-current characteristics of the DC system for sudden decrease in source voltage before and after using SFCL.

SFCL, the voltage-current characteristic exhibit slight oscillations before reaching a new steady state value.

B. SUDDEN LOAD CHANGES

Fig. 8 presents the load voltage and current due to sudden applying load at 0.5 s without SFCL. The load changed from a light load of 300 W to a rated load of 30 kW. As illustrated in the figure, the load voltage increased from 400 V to 480 V with high oscillations in the output voltage. The load voltage reached to steady-state after approximately 40 ms. Also, the load current has a high oscillating response with a first peak of 152 A. on the other hand, Fig. 9 presents the load voltage and current during sudden load change at 0.5 s with applying SFCL. The results illustrate the effectiveness of SFCL to reduce both the oscillation peak and the time. The oscillation peak of the load voltage is reduced to 450 V,

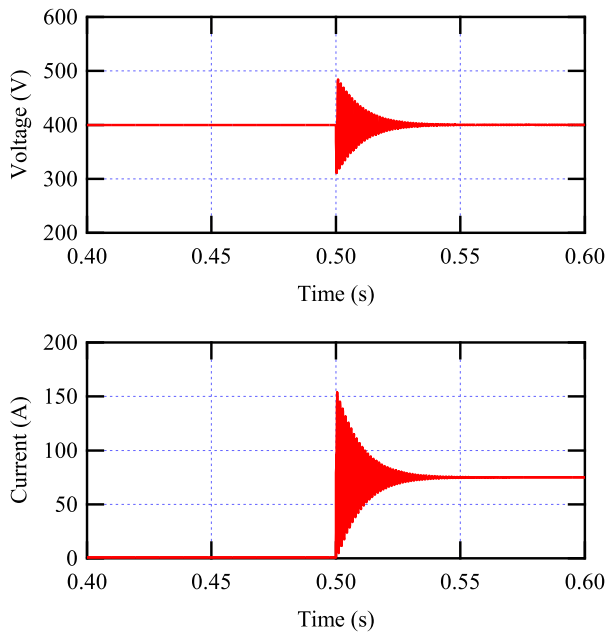


FIGURE 8. Response of DC system for sudden load change before using SFCL.

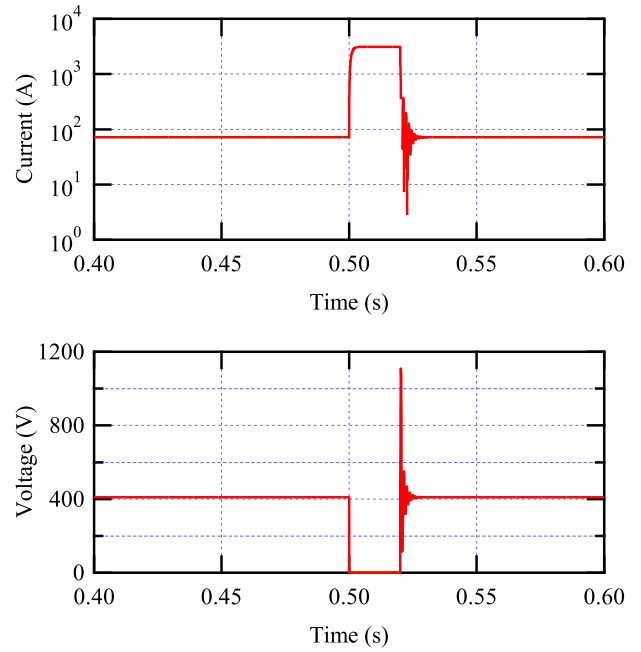


FIGURE 10. Fault response of DC system before using SFCL.

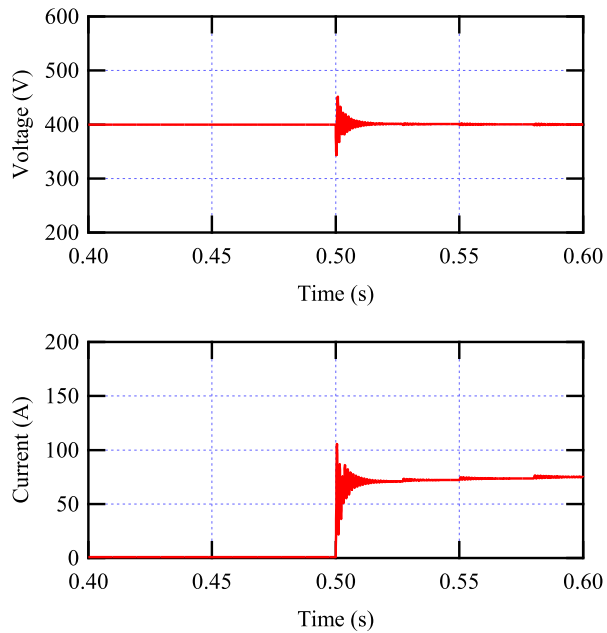


FIGURE 9. Response of DC system for sudden load change after using SFCL.

the maximum peak of the load current is decreased to 105 A, while the oscillation time decreased to about 20 ms. It is clear that SFCL provides high damping for the DC system and suppresses oscillations in both voltage and current.

C. SYSTEM FAULTS

For investigating the impact of SFCL on the performance of DC system against faults, a solid fault case was considered

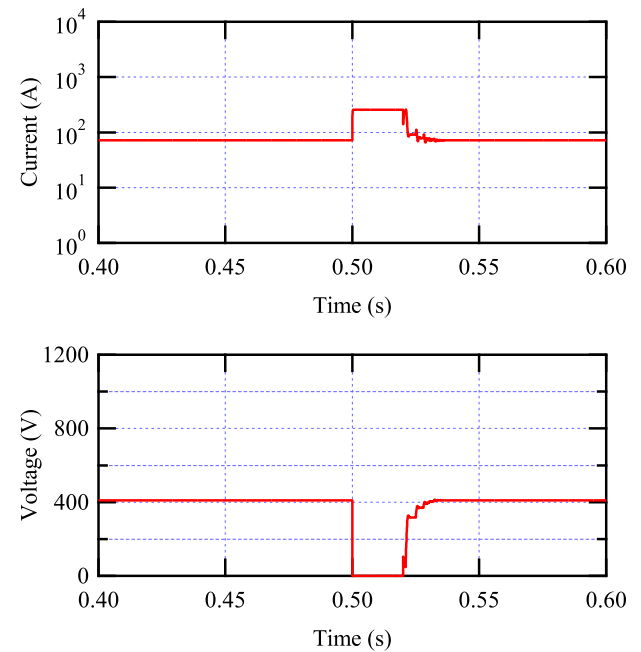


FIGURE 11. Fault response of DC system after using SFCL.

at the load side. The fault instant is 0.5 s and its duration is 20 ms. Without using SFCL in Fig. 10, the fault current increased to a maximum value of about 3.1 kA, which is extremely high. The load voltage decreased to zero during fault and recovered to 400 V after fault clearance. During voltage recovery, an overvoltage occurred and attained about 1100 V before returning to its nominal value after several oscillations persisting for about 5 ms.

After using SFCL in Fig. 11, there is a significant difference in the fault response of the DC system either regarding the maximum fault current or regarding the oscillations following the fault clearance. For maximum fault current, it reached about 260 A. The oscillations in voltage and current after fault clearance were effectively suppressed with no overvoltage occurrence at all.

V. CONCLUSION

In the present study, SFCL was proposed as virtual inertia for DC distribution systems. First, a detailed model for SFCL was built, taking into consideration thermal and electrical issues. Then, the model was implemented with a DC system feeding constant power loads. The stability of the DC system was analyzed using Hurwitz criterion. Different case studies were investigated to validate the effectiveness of SFCL in strengthening the inertia of the DC system. The following conclusions have been reached:

- 1- For the considered transmission line system, the minimum and maximum values of SFCL resistance that achieved voltage stability conditions are 0.5 Ω and 8 Ω , respectively, as obtained from the Hurwitz criterion.
- 2- For step change in the supply voltage, the system exhibits growing oscillations in the load voltage and current, and the system loses stability. By using SFCL, the oscillations were damped effectively, and the system reached a new steady-state value without losing stability.
- 3- For sudden load changes, SFCL could provide high damping for the DC system and suppressed oscillations that occurred in both voltage and current following the load change.
- 4- The fault current reaches very high values without SFCL, and the system undergoes fast transients in the voltage and current after fault clearance. After using SFCL, the system could successfully restore its normal operation after fault clearance without any oscillations, and the fault current was limited effectively.

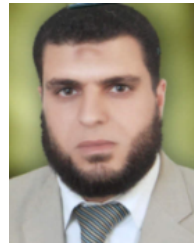
ACKNOWLEDGMENT

The author would like to acknowledge the financial support received from Taif University Researchers Supporting Project Number (TURSP-2020/61), Taif University, Taif, Saudi Arabia.

REFERENCES

- [1] S. A. Asongu, M. O. Agboola, A. A. Alola, and F. V. Bekun, "The criticality of growth, urbanization, electricity and fossil fuel consumption to environment sustainability in Africa," *Sci. Total Environ.*, vol. 712, Apr. 2020, Art. no. 136376.
- [2] S. Saint Akadiri, A. Adewale Alola, G. Olasehinde-Williams, and M. Udom Etokakpan, "The role of electricity consumption, globalization and economic growth in carbon dioxide emissions and its implications for environmental sustainability targets," *Sci. Total Environ.*, vol. 708, Mar. 2020, Art. no. 134653.
- [3] S. Ullah, A. M. A. Haidar, P. Hoole, H. Zen, and T. Ahfock, "The current state of distributed renewable generation, challenges of interconnection and opportunities for energy conversion based DC microgrids," *J. Cleaner Prod.*, vol. 273, Nov. 2020, Art. no. 122777.
- [4] B. Nordman and K. Christensen, "DC local power distribution with microgrids and nanogrids," in *Proc. IEEE 1st Int. Conf. DC Microgrids (ICDCM)*, Jun. 2015, pp. 199–204.
- [5] L. Mackay, N. H. van der Blij, L. Ramirez-Elizondo, and P. Bauer, "Toward the universal DC distribution system," *Electr. Power Compon. Syst.*, vol. 45, no. 10, pp. 1032–1042, 2017.
- [6] D. M. Yehia, Y. Yokomizu, D. Iioka, R. Watanabe, and T. Matsumura, "A novel approach to deliverable power in low-voltage DC distribution system on the basis of voltage stability," *IEEJ Trans. Electr. Electron. Eng.*, vol. 6, no. 5, pp. 395–402, Sep. 2011.
- [7] S. Singh, A. R. Gautam, and D. Fulwani, "Constant power loads and their effects in DC distributed power systems: A review," *Renew. Sustain. Energy Rev.*, vol. 72, pp. 407–421, May 2017.
- [8] M. A. Hassan and Y. He, "Constant power load stabilization in DC microgrid systems using passivity-based control with nonlinear disturbance observer," *IEEE Access*, vol. 8, pp. 92393–92406, 2020.
- [9] Y. Yokomizu, D. M. Yehia, D. Iioka, and T. Matsumura, "Formulated representation for upper limitation of deliverable power in low-voltage DC distribution system," *IEEJ Trans. Power Energy*, vol. 131, no. 4, pp. 362–368, 2011.
- [10] A. Hosseini-pour and H. Hojabri, "Virtual inertia control of PV systems for dynamic performance and damping enhancement of DC microgrids with constant power loads," *IET Renew. Power Gener.*, vol. 12, no. 4, pp. 430–438, Mar. 2018.
- [11] J. Khazaei, Z. Tu, and W. Liu, "Small-signal modeling and analysis of virtual inertia-based PV systems," *IEEE Trans. Energy Convers.*, vol. 35, no. 2, pp. 1129–1138, Jun. 2020.
- [12] Y. Yang, J. Xu, C. Li, T. Dragicevic, and F. Blaabjerg, "Stability enhancement of DC power systems by VSM control strategy," *Int. J. Electr. Power Energy Syst.*, vol. 126, Mar. 2021, Art. no. 106569.
- [13] Y. Yang, C. Li, J. Xu, F. Blaabjerg, and T. Dragicevic, "Virtual inertia control strategy for improving damping performance of DC microgrid with negative feedback effect," *IEEE J. Emerg. Sel. Topics Power Electron.*, vol. 9, no. 2, pp. 1241–1257, Apr. 2021.
- [14] K. Peng, Z. Wei, J. Chen, and H. Li, "Hierarchical virtual inertia control of DC distribution system for plug-and-play electric vehicle integration," *Int. J. Electr. Power Energy Syst.*, vol. 128, Jun. 2021, Art. no. 106769.
- [15] B. Xiang, J. Luo, L. Gao, Z. Liu, Y. Geng, J. Wang, and S. Yanabu, "Study on the parameter requirements for resistive-type superconducting fault current limiters combined with mechanical DC circuit breakers in hybrid AC/DC transmission grids," *IEEE Trans. Power Del.*, vol. 35, no. 6, pp. 2865–2875, Dec. 2020.
- [16] E. W. Nahas, H. A. Abd el-Ghany, D. A. Mansour, and M. M. Eissa, "Extensive analysis of fault response and extracting fault features for DC microgrids," *Alexandria Eng. J.*, vol. 60, no. 2, pp. 2405–2420, Apr. 2021.
- [17] N. Ertugrul and D. Abbott, "DC is the future [Point of view]," *Proc. IEEE*, vol. 108, no. 5, pp. 615–624, May 2020.
- [18] E. W. Nahas, D. A. Mansour, H. A. Abd el-Ghany, and M. M. Eissa, "Developing a smart power-voltage relay (SPV-relay) with no communication system for DC microgrids," *Electr. Power Syst. Res.*, vol. 187, Oct. 2020, Art. no. 106432.
- [19] K. S. Ratnam, K. Palanisamy, and G. Yang, "Future low-inertia power systems: Requirements, issues, and solutions—A review," *Renew. Sustain. Energy Rev.*, vol. 124, May 2020, Art. no. 109773.
- [20] Q. Yang, S. L. Blond, F. Liang, W. Yuan, M. Zhang, and J. Li, "Design and application of superconducting fault current limiter in a multiterminal HVDC system," *IEEE Trans. Appl. Supercond.*, vol. 27, no. 4, Jun. 2017, Art. no. 3800805.
- [21] D. M. Yehia and D. A. Mansour, "Modeling and analysis of superconducting fault current limiter for system integration of battery banks," *IEEE Trans. Appl. Supercond.*, vol. 28, no. 4, Jun. 2018, Art. no. 5603006.
- [22] B. Xiang, L. Gao, Z. Liu, Y. Geng, and J. Wang, "Short-circuit fault current-limiting characteristics of a resistive-type superconducting fault current limiter in DC grids," *Superconductor Sci. Technol.*, vol. 33, no. 2, Jan. 2020, Art. no. 024005.
- [23] D. A. Mansour and D. M. Yehia, "Analysis of 3-phase superconducting fault current limiters in power systems with inhomogeneous quenching," *IEEE Trans. Appl. Supercond.*, vol. 23, no. 3, Jun. 2013, Art. no. 5602605.
- [24] H. J. Schettino, R. D. Andrade Jr, A. Polasek, D. Kottonau, and W. T. B. de Sousa, "A strategy for protection of high voltage systems using resistive superconducting fault current limiters," *Phys. C: Supercond. its Appl.*, vol. 544, pp. 40–45, Jan. 2018.

- [25] S. M. Blair, C. D. Booth, and G. M. Burt, "Current-time characteristics of resistive superconducting fault current limiters," *IEEE Trans. Appl. Supercond.*, vol. 22, no. 2, Apr. 2012, Art. no. 5600205.
- [26] S. Liang, L. Ren, T. Ma, Y. Xu, Y. Tang, X. Tan, Z. Li, G. Chen, S. Yan, Z. Cao, J. Shi, L. Xiao, and M. Song, "Study on quenching characteristics and resistance equivalent estimation method of second-generation high temperature superconducting tape under different overcurrent," *Materials*, vol. 12, no. 15, p. 2374, Jul. 2019.
- [27] B. Li and J. He, "Studies on the application of R-SFCL in the VSC-based DC distribution system," *IEEE Trans. Appl. Supercond.*, vol. 26, no. 3, Apr. 2016, Art. no. 5601005.
- [28] M. H. de Freitas Takami, S. A. Oliveira da Silva, and L. P. Sampaio, "Dynamic performance comparison involving grid-connected PV systems operating with active power-line conditioning and subjected to sudden solar irradiation changes," *IET Renew. Power Gener.*, vol. 13, no. 4, pp. 587–597, Mar. 2019.



IBRAHIM B. M. TAHA received the B.Sc. degree from the Faculty of Engineering, Tanta University, Egypt, in 1995, the M.Sc. degree from the Faculty of Engineering, Mansoura University, Mansoura, Egypt, in 1999, and the Ph.D. degree in electrical power and machines from the Faculty of Engineering, Tanta University, in 2007. Since 1996, he has been a Teaching Staff with the Faculty of Engineering, Tanta University. He joins as an Assistant Professor with the Electrical Engineering Department, Faculty of Engineering, Taif University. He is currently an Associate Professor with Taif University. His research focuses in the area of steady state and transient stability of HVDC systems, FACTS, load forecasting, multi-level inverters, dissolved gas analysis, and artificial intelligent technique applications.

• • •



DOAA M. YEHIA received the B.Sc. and M.Sc. degrees in electrical engineering from Tanta University, Egypt, in 2002 and 2006, respectively, and the Ph.D. degree in electrical engineering from Nagoya University, Nagoya, Japan, in 2011. Since 2003, she has been with the Department of Electrical Power and Machines Engineering, Faculty of Engineering, Tanta University, working as an Instructor, an Assistant Lecturer, and a Lecturer, where she is currently an Assistant Professor. Her research interests include DC distribution systems, renewable energy, energy storage systems, and smart grids.